In Situ Monitoring of the Degradation of Iron Porphyrins by Dioxygen with Hydrazine as Sacrificial Reductant. Detection of Paramagnetic Intermediates in the Coupled Oxidation Process by ^{1}H NMR Spectroscopy

Tamara N. St. Claire and Alan L. Balch*

Department of Chemistry, University of California, Davis, California 95616

Received October 5, 1998

The effects of using hydrazine rather than ascorbic acid on the coupled oxidation of (OEP)$Fe^{II}(py)_2$ (OEP is the dianion of octaethylporphyrin, py is pyridine) have been investigated with the goal of directly detecting reactive intermediates during the process of heme degradation by dioxygen. The reaction products, [(OEOP)$Fe^{II}(py)_2$]Cl and (OEB)$Fe^{III}(py)_2$ (OEOP is the monoanion of octaethyl-5-oxaporphyrin and OEB is the trianion of octaethylbilindione), and their yields are similar to those of the standard coupled oxidation process. The reaction has been monitored *in situ* in pyridine/dichloromethane mixtures by ^{1}H NMR spectroscopy. The recently isolated and crystallographically characterized complex, (OEPO)$Fe(py)_2$ (OEOP is the trianion of octaethyloxaphlorin), has been identified as a key intermediate. Addition of dioxygen to (OEP)$Fe^{II}(py)_2$ in pyridine with hydrazine present also produces two new transient species: (OEPO)$Fe(py)(N_2D_4)$ and (OEPO)$Fe(N_2D_4)_2$. These complexes have also been produced independently by low-temperature titration of hydrazine into a solution of $\{$(OEPO)Fe$\}_2$. Thus, hydrazine acts as an axial ligand during the early stages of the coupled oxidation process. However, the two hydrazine-containing complexes eventually are converted into (OEPO)$Fe(py)_2$ before [(OEOP)$Fe^{II}(py)_2$]Cl and (OEB)$Fe^{III}(py)_2$ are formed. The observations reported here suggest that the coupled oxidation process can be divided into two stages. The first stage involves the meso C−H bond and results in introduction of oxygen at that site with the formation of the three intermediates: (OEPO)$Fe(N_2H_4)_2$, (OEPO)$Fe(N_2H_2)$(py), and (OEPO)-$Fe(py)_2$. The second stage of the coupled oxidation process involves C−C bond breaking and the conversion of the hydroxylated heme, (OEPO)$Fe(py)_2$, into the final products, [(OEOP)$Fe^{II}(py)_2]^+$ and (OEB)$Fe^{III}(py)_2$.

Introduction

Biological heme degradation is catalyzed by two enzymes, heme oxygenase and biliverdin reductase as shown in Scheme 1.[1] Heme oxygenase utilizes dioxygen to cleave heme specifically at the α methine position and to remove one carbon atom, which is converted into carbon monoxide, a suspected neurotransmitter.[2] The blue/green pigment, biliverdin, and iron ions are also released in this process. Biliverdin is subsequently reduced to bilirubin, the yellow pigment that is responsible for jaundice in humans.

The coupled oxidation process, in which heme degradation is brought about by dioxygen in the presence of a reducing agent (generally ascorbic acid) has been widely employed as a model for biological heme catabolism.[3,4] The coupled oxidation procedure can be utilized to oxidize iron porphyrins as model compounds or to oxidize intact heme proteins. Results from this laboratory have shown that coupled oxidation of the model compound, (OEP)$Fe^{II}(py)_2$ (py is pyridine, OEP is the dianion of octaethylporphyrin), produces not only the previously observed verdoheme[5] but also an iron(III) biliverdin complex as shown in Scheme 2.[6] Octaethylverdoheme, a green, diamagnetic complex of iron(II), has recently been characterized by a single-crystal X-ray diffraction study and shown to contain the planar 5-oxaporphyrin macrocycle.[7] A number of other iron complexes of the 5-oxaporphyrin ligand have also been carefully characterized in terms of oxidation, ligation, and spin states.[5,8] The iron biliverdin complex, (OEB)$Fe^{III}(py)_2$, is a high-spin species that is easily identified on the basis of its paramagnetically shifted ^{1}H NMR spectrum. Upon removal of pyridine, this complex undergoes dimerization to form $\{$(OEB)$Fe^{III}\}_2$. Other related work has shown that coupled oxidation of (OEP)Fe^{II} can be conducted in methanol with cyanide replacing pyridine as an axial ligand,[9] and that (OEP)Co^{II} undergoes coupled oxidation in dichloromethane/tetrahydrofuran mixtures to form 5-oxaporphyrin- and biliverdin-derived compounds.[10,11] While coupled oxidation of heme alone produces a mixture of all four

(1) (a) Maines, M. D. *Heme Oxygenase: Clinical Applications and Functions*; CRC Press: Boca Raton, FL, 1992 (b) O'Carra, P. In *Porphyrins and Metalloporphyrins*; Smith, K. M., Ed.; Elsevier: New York, 1975; p 123. (c) Schmid, R.; McDonagh, A. F. In *The Porphyrins;* Dolphin, D., Ed.; Academic Press: New York, 1979; Vol. 6, p 258. (d) Bissel, D. M. In *Liver: Normal Function and Disease*; Ostrow, J. D., Ed.; Marcel Dekker, Inc.: New York, 1986; Vol. 4, Bile Pigments and Jaundice, p 133. (e) Beale, S. I. *Chem. Revs.* **1993**, *93*, 785.
(2) Verma, A.; Hirsch, D. J.; Glatt, G. E.; Ronnett, G. V.; Snyder, S. H. *Science* **1993**, *259*, 381.
(3) Warburg, O.; Negelein, E. *Chem. Ber.* **1930**, *63*, 1816.
(4) Lagarias, J. C. *Biochim. Biophys. Acta* **1982**, *717*, 12.
(5) Balch, A. L.; Latos-Grażyński, L.; Noll, B. C.; Olmstead, M. M.; Szterenberg, L.; Safari, N. *J. Am. Chem. Soc.* **1993**, *115*, 1422.
(6) Balch, A. L.; Latos-Grażyński, L.; Noll, B. C.; Olmstead, M. M.; Safari, N. *J. Am. Chem. Soc.* **1993**, *115*, 9056.
(7) Balch, A. L.; Koerner, R.; Olmstead, M. M. *J. Chem. Soc., Chem. Commun.* **1995**, 873.
(8) Balch, A. L.; Noll, B. C.; Safari, N. *Inorg. Chem.* **1993**, *32*, 2901.
(9) Balch, A. L.; Koerner, R.; Latos-Grażyński, L.; Lewis, J. E.; St. Claire, T. N.; Zovinka, E. P. *Inorg. Chem.* **1997**, *36*, 3892.
(10) Balch, A. L.; Mazzanti, M.; Olmstead, M. M. *J. Chem. Soc., Chem. Commun.* **1994**, 269.
(11) Balch, A. L.; Mazzanti, M.; St. Claire, T. N.; Olmstead, M. M. *Inorg. Chem.* **1995**, *34*, 2194.

10.1021/ic981178d CCC: $18.00
Published on Web 01/28/1999

Scheme 1. Biological Heme Degradation

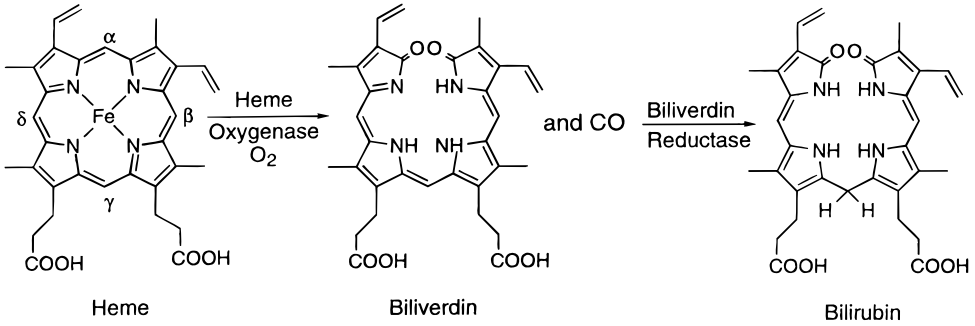

Scheme 2. Coupled Oxidation of Heme

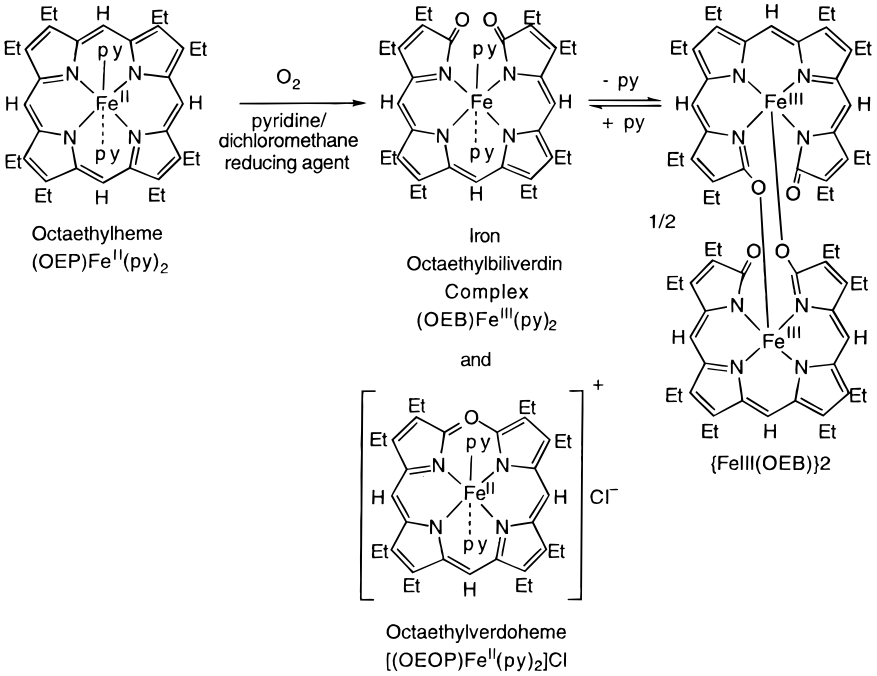

biliverdin isomers as a result of reaction at all four meso positions;[12] coupled oxidation of myoglobin, as well as an active site variant, results in exclusive cleavage at the α meso carbon.[13,14]

It is widely accepted that the first step in heme degradation by heme oxygenase results in the meso hydroxylation of the heme.[1c,15−19] The major evidence for initial heme hydroxylation has come from studies that show that α-hydroxylated heme binds to heme oxygenase and can replace heme as a substrate for heme oxygenase. However, only recently has direct spectroscopic evidence been produced that suggests that a meso-hydroxylated heme is formed by heme oxygenase.[20] For coupled oxidation of $(OEP)Fe^{II}(py)_2$, meso hydroxylation would be expected to produce $(OEPO)Fe(py)_2$, a compound which has received considerable study,[21−24] and which has recently been isolated in pure form in this laboratory.[25] $(OEPO)Fe(py)_2$ is conveniently prepared by the addition of pyridine to the dimer, $\{(OEPO)Fe^{III}\}_2$,[26] in the absence of dioxygen as shown in Scheme 3.[27] While the crystallographic data on this species indicate that the iron is in a high spin state, the assignment of the iron and ligand oxidation states in this complex is less clear, since it can exist in any of the three combinations of oxidation states shown in Scheme 3. Spectroscopically, $(OEPO)Fe(py)_2$ is readily identified on the basis of its characteristic ^1H NMR spectrum which displays marked upfield shifts for the two types of meso protons and both upfield and downfield shifts for the methylene protons.

(12) Bonett, R.; McDonagh, A. F. *J. Chem. Soc., Perkin Trans. I* **1973**, 881.
(13) O'Carra, P.; Colleran, E. *FEBS Lett.* **1969**, *5*, 295.
(14) Hildebrand, D. P.; Tang, H.: Luo, Y.; Hunter, C. L.; Smith, M.; Brayer, G. D.; Mauk, A. G. *J. Am. Chem. Soc.* **1996**, *118*, 12909.
(15) Yoshida, T.; Noguchi, M.; Kikuchi, G.; Sano, S. *J. Biochem.* **1981**, *90*, 125.
(16) Sano, S.; Sano, T.; Morishima, I.; Shiro, Y.; Maeda, Y. *Proc. Natl. Acad. Sci. U.S.A.* **1986**, *83*, 531.
(17) Wilks, A.; Ortiz de Montellano, P. R. *J. Biol. Chem.***1993**, *268*, 22357.
(18) Wilks, A.; Torpey, J.; Ortiz de Montellano, P. R. *J. Biol. Chem.***1994**, *269*, 29553.
(19) Mansfield Matera, K.; Takahashi, S.; Fujii, H.; Zhou, H.; Ishikawa, K.; Yoshimura, T.; Rousseau, D. L.; Yoshida, T.; Ikeda-Saito, M. *J. Biol. Chem.***1996**, *271*, 6618.
(20) Liu, Y.; Moënne-Loccoz, P.; Loehr, T. M.; Ortiz de Montellano, P. R. *J. Biol. Chem.* **1997**, *272*, 6909.
(21) Sano, S.; Sugiura, Y.; Maeda, Y.; Ogawa, S.; Morishima, I. *J. Am. Chem. Soc.* **1981**, *103*, 2888.
(22) Morishima, I.; Fujii, H.; Shiro, Y. *J. Am. Chem. Soc.* **1986**, *108*, 3858.
(23) Morishima, I.; Shiro, Y. Hiroshi, F. *Inorg. Chem.* **1995**, *34*, 1528.
(24) Balch, A. L.; Noll, B. C.; Reid, S. M.; Zovinka, E. P. *Inorg. Chem.* **1993**, *32*, 2610.
(25) Balch, A. L.; Koerner, R.; Latos-Grażyński, L.; Noll, B. C. *J. Am. Chem. Soc.* **1996**, *118*, 2760.
(26) Balch, A. L.; Latos-Grażyński, L.; Noll, B. C.; Olmstead, M. M.; Zovinka, E. P. *Inorg. Chem.* **1992**, *31*, 2248.
(27) Balch, A. L.; Noll, B. C.; Reid, S. M.; Zovinka, E. P. *Inorg. Chem.* **1993**, *32*, 2610.

Scheme 3

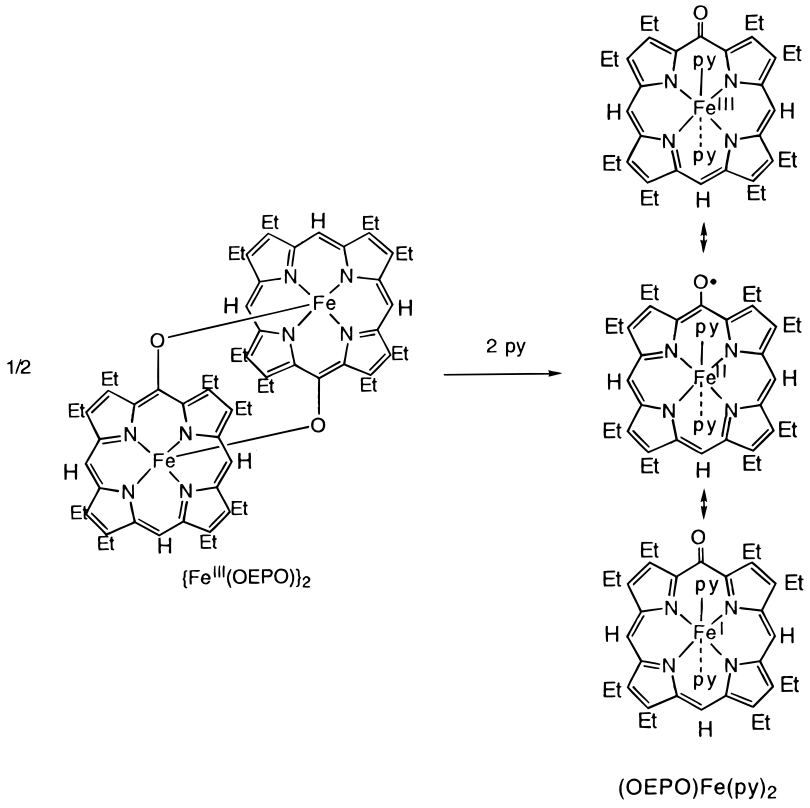

Table 1. ^{1}H NMR Parameters for Iron Complexes

compound	spin state	coordination no.	meso	methylene	methyl	solvent	*T*, °C	ref
(OEP)Fe^{III}Cl	$^5/_2$	5	−34	42, 45	7	py	20	*a*
(OEP)Fe^{III}Cl(py)	$^5/_2$	5,6	∼0	53, 58	7		−30	
{(OEP)Fe^{III}}$_2$O	$^5/_2$[i]	5	5.5	6.06, 5.10	1.75	$CDCl_3$	29	*b*
{(OEP)Fe^{III}O}$_2$	$^5/_2$[i]	5	−2.3	8.85, 6.26	1.74	toluene-d_8	−75	*c*
(OEP)(*N*-MeIm)Fe^{IV}=O	1	6	15	0	3.2	toluene-d_8	−33	*d*
(OEP)Fe^{II}	1	4	76.3	33.8	12.9	benzene-d_6	25	*e*
[(OEOP)Fe^{II}(py)$_2$]Cl	0	6	9.6(2)	3.63, 3.51	1.67, 1.63	py	−30	*f*
			9.1(1)	3.42 3.40	1.61, 1.55			
(OEB)Fe^{III}(py)$_2$	5/2	6	39.5	80, 67	0−6	py	−30	*g*
			∼30	52, 24				
(OEPO)Fe(py)$_2$	high	6	−198	30		py	−30	*h*
			−141	−9				

[a] Morishima, I.; Kitagawa, S.; Matsuki, E.; Inubushi, T. *J. Am. Chem. Soc.* **1980**, *102*, 2429. [b] La Mar, G. N.; Eaton, G. R.; Holm, R. H.; Walker, F. A. *J. Am. Chem. Soc.* **1973**, *95*, 63. [c] Chin, D. H.; La Mar, G. N.; Balch, A. L. *J. Am. Chem. Soc.* **1980**, *102*, 4344. [d] La Mar, G. N.; deRopp, J. S.; Latos-Grażyński, L.; Balch, A. L.; Johnson, R. B.; Smith, K. M.; Parish, D. W.; Cheng, R.-J. *J. Am. Chem. Soc.* **1983**, *105*, 782. [e] Strauss, S. H.; Silver, M. E.; Long, K. M.; Thompson, R. G.; Hudgens, R. A.; Spartalian, K.; Ibers, J. A. *J. Am. Chem. Soc.* **1985**, *107*, 4207. [f] Balch, A. L.; Latos-Grażyński, L.; Noll, B. C.; Olmstead, M. M.; Szterenberg, L.; Safari, N. *J. Am. Chem. Soc.* **1993**, *115*, 1427. [g] Balch, A. L.; Latos-Grażyński, L.; Noll, B. C.; Olmstead, M. M.; Safari, N. *J. Am. Chem. Soc.* **1993**, *115*, 9056. [h] Balch, A. L.; Koerner, R.; Latos-Grażyński, L.; Noll, B. C. *J. Am. Chem. Soc.* **1996**, *118*, 2760. [i] Two antiferromagnetically coupled $S = {}^5/_2$ Fe(III) cnters.

Here we present a set of experimental results on the direct detection of intermediates during the coupled oxidation process. To accomplish this, we have chosen to utilize hydrazine rather than the more generally employed ascorbic acid as the sacrificial reducing agent in this reaction. Hydrazine is available in deuterated form and the use of hydrazine-d_4 simplifies the acquisition of suitable ^{1}H NMR spectra by avoiding having the reducing agent provide a overwhelming contribution to the overall NMR spectral intensity. Hydrazine and phenyl hydrazine have previously been employed in the coupled oxidation process, but verdoheme was the only product characterized in these reactions.[28,29]

(28) Itano, H. A.; Hirota, T. *Biochem. J.* **1985**, *226*, 767.
(29) Hirota, T.; Itano, H. A. *Tetrahedron Lett.* **1983**, *24*, 995.

Results

Isolation of the Products from the Coupled Oxidation of {(OEP)Fe^{II}(py)$_2$} with Hydrazine as Reductant. To verify that the use of hydrazine rather than ascorbic acid does not alter the products of coupled oxidation, the reaction was run on a preparative scale so that the final products could be isolated and identified. The procedure developed earlier in this laboratory was utilized with hydrazine replacing the ascorbic acid. Product identification was facilitated by the use of the spectral data for relevant iron complexes that are shown in Table 1. Addition of dioxygen to a partially frozen dichloromethane/pyridine solution of (OEP)Fe^{II}(py)$_2$ and hydrazine produces a green solution. The electronic absorption spectrum and green color are indicative of the formation of the verdoheme, [(OEOP)Fe^{II}(py)$_2$]Cl. This

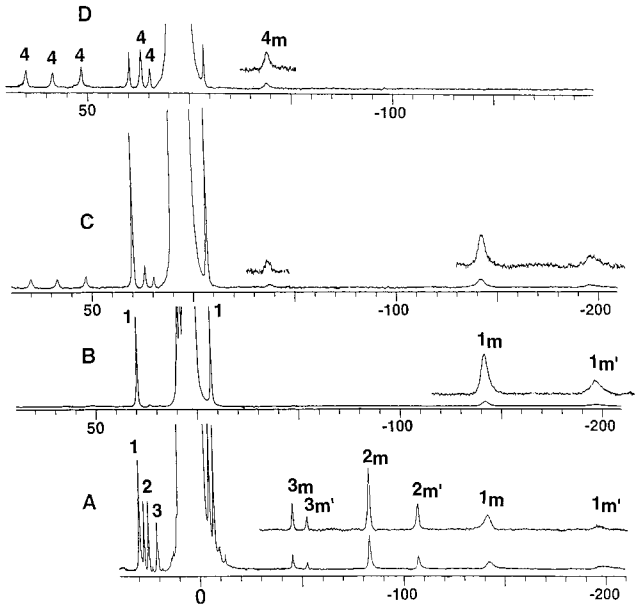

Figure 1. 300 MHz ^{1}H NMR spectra from the reaction of (OEP)Fe^{II}(py)$_2$ in dichloromethane-d_2/pyridine-d_5 (6.7/1 v/v) with hydrazine-d_4 at −30 °C: (trace A) immediately after the addition of dioxygen; (trace B) after 10 min at −30 °C; (trace C) after the NMR tube is shaken for 30 s and placed back in the −30 °C probe; (trace D) after an additional 20 min has elapsed. The resonances of (OEPO)Fe(py)$_2$, (OEPO)Fe(py)(N_2D_4) and (OEPO)Fe(N_2D_4)$_2$ are labeled **1**, **2**, and **3** respectively. Subscripts m and m′ designate the resonances from the meso protons.

salt was removed by precipitation with *n*-hexane and obtained in a 42% yield. The identity of the product was confirmed by observation of its ^{1}H NMR spectrum. After chromatography (in an inert atmosphere) of the solution that remained after removal of [(OEOP)Fe^{II}(py)$_2$]Cl, {(OEB)Fe^{III}}$_2$ was obtained in a 22% yield. Again the identity of the product was confirmed by comparison of the ^{1}H NMR and UV/vis spectra with those of an authentic sample.

***In Situ* Monitoring of the Coupled Oxidation Process by ^{1}H NMR Spectroscopy.** The addition of dioxygen to a solution of (OEP)Fe^{II}(py)$_2$ and hydrazine in dichloromethane-d_2/pyridine-d_5 (13/87 v/v) was monitored by ^{1}H NMR spectroscopy at −30 °C. Figure 1 shows the relevant data for the reaction. The data are presented so that all paramagnetic resonances are visible, but the resonances in the 10 to 0 ppm region, in which resonances of diamagnetic compounds occur, have been truncated.

Initially, when hydrazine-d_4 alone is added to the solution of (OEP)Fe^{II}(py)$_2$, there is no change in the ^{1}H NMR spectrum and no paramagnetically shifted resonances are observed. Trace A in Figure 1 shows the spectrum immediately after the subsequent addition of dioxygen to the sample of (OEP)Fe^{II}(py)$_2$ with hydrazine-d_4 present. An array of paramagnetically shifted resonances is apparent. These resonances are assigned to three discreet species: **1**, **2**, and **3**. Throughout the reaction, the relative intensities of the resonances assigned to **1** remained constant. Similarly the relative intensities the resonances assigned to **2** (and to **3**) remained constant, although the relative amounts of **1**, **2**, and **3** varied as the reaction progressed. The resonances labeled **1,** with two meso resonances shifted far upfield and two distinctive methylene resonances at ca. 30 ppm and −10 ppm, are unambiguously assigned on the basis of their chemical shifts and relative intensities to the previously characterized complex, (OEPO)Fe(py)$_2$ (*vide infra* to Trace A in Figure 2).

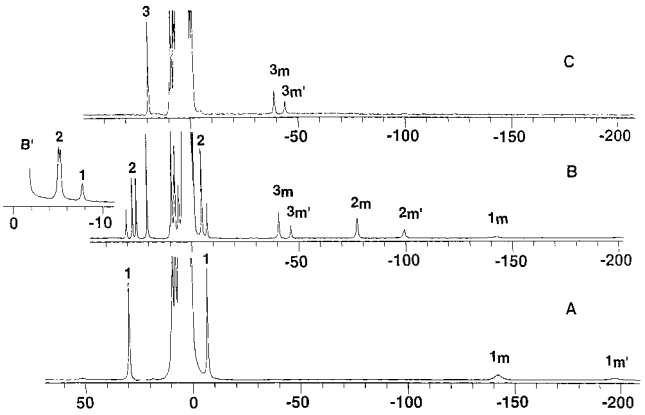

Figure 2. 300 MHz ^{1}H NMR spectra from the reaction of (OEPO)Fe(py)$_2$ in pyridine-d_5 with hydrazine-d_4 at −30 °C: (trace A) before the addition of hydrazine-d_4; (trace B) after the addition of 18 equiv of hydrazine-d_4; (trace C) after the addition of 72 equiv of hydrazine-d_4.. The resonances are labeled following the scheme used in Figure 1.

The patterns of resonances for the other two species are similar with two resonances in a 2:1 intensity ratio shifted upfield and additional resonances in the 30 to −10 ppm range that are due to the methylene protons. These changes are consistent with what would be expected for the formation of an iron oxophlorin species with unique axial ligation. On the basis of similarity in patterns of resonances (and the data in the following section), we ascribe these new features in the ^{1}H NMR spectrum to the formation of the six-coordinate complexes, (OEPO)Fe(py)(N_2D_4) (resonances labeled **2**) and (OEPO)Fe(N_2D_4)$_2$ (resonances labeled **3**).

Trace B of Figure 1 shows spectrum of the sample at −30 °C after 10 minutes have elapsed. The resonances labeled **2** and **3** and assigned to (OEPO)Fe(py)(N_2D_4) and (OEPO)Fe(N_2D_4)$_2$, respectively, cannot be detected. However the resonances (labeled **1**) of (OEPO)Fe(py)$_2$ are still present.

Trace C shows the spectrum of the sample after the NMR tube was shaken for thirty seconds at room temperature and placed back in the −30 °C probe. The dominant species is still (OEPO)Fe(py)$_2$, but the appearance of new resonances shows that another product is beginning to appear.

Trace D shows the sample after another 20 min has elapsed. The resonances of the new product have grown in intensity while the resonances of (OEPO)Fe(py)$_2$ are lost. The new product is readily identified as (OEB)Fe^{III}(py)$_2$ through comparison of these spectral features with those of an authentic sample.[6] Only one of the two meso resonances of (OEB)Fe(py)$_2$ is observed. At this temperature this resonance appears at −39 ppm, while the other meso resonance, which is expected at ca. 30 ppm, is broadened beyond detection. Seven of the eight methylene resonances are observable in the paramagnetic spectrum. The eighth resonance is hidden in the diamagnetic region at 3.5 ppm.

An electronic absorption spectrum was taken of a diluted sample of the reaction mixture at this stage of the reaction. That spectrum is shown in Figure S1 (See Supporting Information). The spectral features are consistent with the production of the verdoheme, [(OEOP)Fe^{II}(py)$_2$]Cl, which is not detected in the ^{1}H NMR spectra shown in Figure 1 because of its diamagnetic nature. The spectral features of (OEB)Fe^{III}(py)$_2$ are not observed in the UV/vis spectrum because it is produced in a smaller yield and its molar absorptivities are lower than those of [(OEOP)Fe^{II}(py)$_2$]Cl. In addition, its UV/vis spectrum is broad and less distinctive than that of [(OEOP)Fe^{II}(py)$_2$]Cl. Thus the spectral features of (OEB)Fe(py)$_2$ are hidden beneath the verdoheme absorbances.

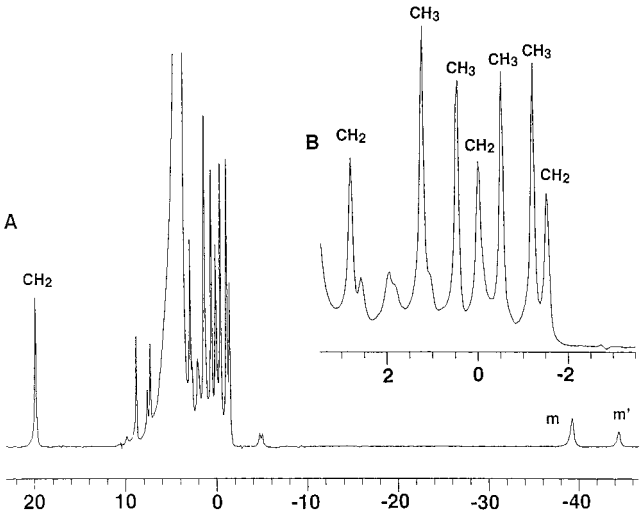

Figure 3. The 300 MHz ^{1}H NMR spectrum of (OEPO)Fe(N_2D_4)$_2$ at −40 C. Meso protons are identified by m and m′, methylene resonances are identified by CH_2, and methyl resonances are denoted by CH_3. When this spectrum is taken under inversion recovery conditions, the resonances in the 10 to 3 ppm region are inverted. Thus they are due to residual protons in the solvents.

No further changes were seen in either the ^{1}H NMR or the UV/vis spectra of the reaction mixture beyond this point in time.

Reaction of (OEPO)Fe(py)$_2$ with Hydrazine in Pyridine Solution. The addition of hydrazine at −30 °C to (OEPO)Fe(py)$_2$ produces the same two new species, (OEPO)Fe(py)(N_2D_4) and (OEPO)Fe(N_2D_4)$_2$, that are observed during the coupled oxidation reaction described above. Figure 2 shows relevant data for the titration. Trace A shows a sample of (OEPO)Fe(py)$_2$ in pyridine-d_5 before the addition of hydrazine-d_4. Trace B shows the spectrum of the sample after the addition of 18 equiv (relative to the initial (OEPO)Fe(py)$_2$ concentration) of hydrazine-d_4. Resonances due to (OEPO)Fe(py)$_2$ begin to diminish in intensity as the resonances of two new species (labeled **2** and **3**) develop.

Trace C shows the sample after a total of 72 equiv of hydrazine-d_4 have been added. The resonances from (OEPO)Fe(py)$_2$ (**1**) and (OEPO)Fe(py)(N_2D_4) (**2**) have been replaced by those for the symmetrically ligated species, (OEPO)Fe(N_2D_4)$_2$ (**3**). Since the proportions of **1**, **2**, and **3** that are present can be controlled by controlling the hydrazine concentration, we believe that these three compounds are in equilibrium with free hydrazine and pyridine.

Figure 3 shows the spectrum of (OEPO)Fe(N_2D_4)$_2$ so that all the resonances can be seen. The spectrum shows the meso protons, m and m′, at −39 and −44 ppm with a 2:1 intensity ratio. The methylene protons, labeled CH_2, appear at 19.7, 2.8, −0.1, and −1.6 ppm. Inset B shows an expansion of the methylene and methyl region. There are four methyl resonances labeled CH_3 in the 2 to −2 ppm range. All of these resonances have the appropriate integrated intensities which has facilitated their assignment. The spectral features are consistent with the formulation of the complex as (OEPO)Fe(N_2D_4)$_2$ with symmetrical ligation on either side of the plane of the tetrapyrrole ligand.

While four methylene resonances are expected for (OEPO)Fe(N_2D_4)$_2$, eight methylene resonances are expected for (OEPO)Fe(py)(N_2D_4) where the ligation about the plane of the OEOP portion is unsymmetrical. Unfortunately since (OEPO)Fe(py)(N_2D_4) is always formed in the presence of some (OEPO)Fe(py)$_2$ or (OEPO)Fe(N_2D_4)$_2$, it has not been possible to clearly identify all of the methylene and methyl resonances of this complex. Trace B of Figure 3 shows that there are a pair of downfield methylene resonances at ca. 27 ppm that are assigned to (OEPO)Fe(py)(N_2D_4), whereas both (OEPO)Fe(py)$_2$ and (OEPO)Fe(N_2D_4)$_2$ display only a single methylene resonance in this region due to their higher symmetry. An MCOSY spectrum, which is useful for the identification of resonances from an individual ethyl group in a paramagnetic heme,[30] shows that the two equally intense resonances at ca. 27 ppm are indeed coupled to one another and to a methyl resonance at 1.3 ppm. The inset B′ in Figure 2 shows that the upfield methylene resonance assigned to (OEPO)Fe(py)(N_2D_4) is split into a doublet when the sample is cooled to −40 °C. The remaining methylene and methyl resonances of (OEPO)Fe(py)(N_2D_4) are likely within the crowded diamagnetic region as is also the case with other complexes of this type.

The behavior of the meso resonances with changes in the axial ligation correlates well with previous observations of complexes of the type (OEPO)Fe(L)$_2$ with different axial ligands (L).[23] That work showed that an increase in axial ligand pK_a value resulted in a downfield shift to the meso resonances.[23] Additionally, the line width of the meso resonances narrowed as the ligand pK_a values increased. The same trend is seen here where the pK_a value for pyridine is 5.28 while that of hydrazine is 8.32. Thus the meso resonances of (OEPO)Fe(py)(N_2D_4) are shifted downfield of those of (OEPO)Fe(py)$_2$ and those of (OEPO)Fe(N_2D_4)$_2$ are shifted even further downfield. Similarly the line widths of the meso resonances decreases in the order: (OEPO)Fe(py)$_2$ > (OEPO)Fe(py)(N_2D_4) > (OEPO)Fe(N_2D_4)$_2$.

The effects of temperature on the ^{1}H NMR spectra of (OEPO)Fe(py)(N_2D_4) and (OEPO)Fe(N_2D_4)$_2$ are shown in Figures S2 and S3 (see Supporting Information) where the chemical shifts for the two upfield meso resonances and the downfield methylene resonance(s) are plotted versus 1/T. For a paramagnetic complex, these plots reveal rather small effects of temperature on the chemical shifts even in comparison of the Curie plots with that for (OEPO)Fe(py)$_2$. The non-Curie temperature dependence of these spectra may arise from the unusual electronic structures of this family of species which can have magnetic coupling between ligand and metal based electrons.

Attempts to isolate the new species, (OEPO)Fe(py)(N_2D_4) and (OEPO)Fe(N_2D_4)$_2$, have not been successful. Reduction by hydrazine at ambient temperatures appears to be a problem.

A sample of (OEPO)Fe(py)$_2$ was also titrated with 1,1-dimethylhydrazine in an attempt to replace the axial pyridine ligands with another hydrazine. However, addition of 1,1-dimethylhydrazine to (OEPO)Fe(py)$_2$ in pyridine-d_5 produced no changes in the ^{1}H NMR spectrum either at room temperature or at −30 °C. We also examined the affects of additions of 1,1-dimethylhydrazine to {(OEPO)Fe}$_2$ in dichloromethane-d_2 and chloroform-d, but again no changes were observed in the ^{1}H NMR spectra of the samples. The inability of 1,1-dimethylhydrazine to replace pyridine as an axial ligand is probably a result of a steric effect.

Reactions of Iron Porphyrins with Oxidants in the Absence of Hydrazine. The reactivities of iron porphyrins toward oxidants under the conditions utilized in this work, but without hydrazine present, have been examined in order to further identify plausible reactions in the coupled oxidation process. Without hydrazine, solutions of (OEP)Fe^{II}(py)$_2$ in pyridine are stable for several hours toward oxidation by

(30) Keating, K. A.; de Ropp, J. S.; La Mar, G. N.; Balch, A. L.; Shiau, F. Y.; Smith, K. M. *Inorg. Chem.* **1991**, *30*, 3258.

dioxygen at both −30 °C and at room temperature. However, treatment of a sample of $(OEP)Fe^{II}(py)_2$ in pyridine with hydrogen peroxide under strictly anaerobic conditions cleanly produces $(OEPO)Fe(py)_2$. In this case the reaction has been monitored by ^1H NMR spectroscopy, and a spectrum analogous to that shown in Trace A of Figure 3 was obtained. Although $(OEPO)Fe(py)_2$ is tolerant of the presence of an excess of hydrogen peroxide, it is quite reactive toward dioxygen. When a solution of $(OEPO)Fe(py)_2$ that is prepared either by addition of hydrogen peroxide to a pyridine solution of $(OEP)Fe(py)_2$ or by dissolution of $\{(OEPO)Fe^{III}\}_2$ in pyridine, is treated with dioxygen, it is converted into the verdoheme, $[(OEOP)Fe^{II}(py)_2]^+$, and the biliverdin complex, $(OEB)Fe^{III}(py)_2$. When either of these reactions is monitored by ^1H NMR spectroscopy, the spectrum of the resulting solution resembles that shown in Trace D of Figure 1 (which shows that $(OEB)Fe^{III}(py)_2$ is present), while the UV/vis spectrum of the solution reveals that green $[(OEOP)Fe^{II}(py)_2]Cl$ is present. On the other hand, the ^1H NMR spectrum of $(OEP)Fe^{III}Cl$ in pyridine-d_5 at −30 °C (methylene protons at 52 and 57 ppm, meso protons at ca. 0 ppm) is unaffected by the addition of either dioxygen or hydrogen peroxide.

Discussion

The results presented here give considerable insight into the process of coupled oxidation. With $(OEP)Fe^{II}(py)_2$ and hydrazine that process produces the same products, $[(OEPO)Fe^{II}(py)_2]^+$ and $\{(OEB)Fe^{III}\}_2$ that are formed when ascorbic acid is used as reductant. The variation in isolated product yield (50% for $[(OEPO)Fe^{II}(py)_2]Cl$, 32% for $\{(OEB)Fe^{III}\}_2$ with ascorbic acid; 42% for $[(OEPO)Fe^{II}(py)_2]Cl$, 22% for $\{(OEB)Fe^{III}\}_2$ with hydrazine) is not considered to be significant. The procedure previously developed with ascorbic acid was simply modified to use hydrazine without further optimization of conditions, and $\{(OEB)Fe^{III}\}_2$ is known to be unstable during the process of its isolation.

The role of hydrazine in the coupled oxidation process is complex. Hydrazine forms a number of transition metal compounds where it can act as monodentate, bidentate, or bridging ligand,[31] and it acts as a ligand in forming the intermediates $(OEPO)Fe(N_2D_4)_2$ and $(OEPO)Fe(N_2D_4)(py)$ that we have observed. In these complexes, the hydrazine is almost certainly acting as a monodentate ligand since it simply replaces pyridine. In this regard, there is the possibility that the coupled oxidation of model compounds with hydrazine differs significantly from the process that occurs in heme oxygenase. However, it should also be recognized that another major difference exists between the coupled oxidation process and the reaction catalyzed by heme oxygenase. The former process produces cleavage at all four meso sites in protoheme while heme oxygenase produces only one biliverdin isomer.

It is important to note that hydrazine also can act as a reductant and can react with dioxygen in a complex series of reactions.[32,33] Not only can hydrazine reduce dioxygen to form water as shown in eq 1, but it also forms hydrogen peroxide during the autoxidation process as seen in eq 2. Thus throughout the initial stages of the coupled oxidation process, hydrazine can be lost through oxidation which can generate hydrogen peroxide.

$$O_2 + N_2H_4 \rightarrow 2H_2O + N_2 \quad (1)$$

$$2O_2 + N_2H_4 \rightarrow 2H_2O_2 + N_2 \quad (2)$$

The observations reported here suggest that the coupled oxidation process can be divided into two stages as shown in Scheme 4. The first stage is a multistep process that involves meso C−H bond activation and results in introduction of oxygen at that site. That stage results in the formation of the three intermediates: $(OEPO)Fe(N_2H_4)_2$, $(OEPO)Fe(N_2H_2)(py)$, and $(OEPO)Fe(py)_2$. Under the conditions of our experiments these species appear to be in equilibrium with one another. The latter of these is sufficiently stable to be isolated and fully characterized,[25] while the other two are only stable in solution under controlled conditions. Nevertheless, $(OEPO)Fe(N_2H_4)_2$ and $(OEPO)Fe(N_2H_4)(py)$ have been prepared independently by treatment of $(OEPO)Fe(py)_2$ with hydrazine. The first stage also appears to involve hydrogen peroxide, not dioxygen itself as the oxidant. As demonstrated here and elsewhere,[21,25] $(OEPO)Fe(py)_2$ can be obtained cleanly through the reaction of $(OEP)Fe^{II}(py)_2$ and hydrogen peroxide *under anaerobic conditions*, but it is not formed from $(OEP)Fe^{II}(py)_2$ and dioxygen alone. Notice that the hydrazine-containing intermediates, $(OEPO)Fe(N_2H_4)_2$ and $(OEPO)Fe(N_2H_4)(py)$, disappear before we see signs of the formation of $(OEB)Fe^{III}(py)_2$ (see Traces A, B, and C of Figure 1). These changes are probably due to the decrease in hydrazine concentration at this late stage of the reaction. During the initial stages, the presence of hydrazine also protects these intermediates from further attack by dioxygen presumably through reduction of O_2 (i.e., via eq 1). Nevertheless, the presence of hydrazine as reductant in the first stage of the coupled oxidation process has provided conditions in which the $(OEPO)FeL_2$ unit survives despite the introduction of dioxygen into the system. It is also significant that treatment of heme oxygenase with hydrogen peroxide under anaerobic conditions has been shown to produce a meso-oxygenated heme analogous to $(OEPO)Fe(py)_2$ as a detectable intermediate.[20]

The second stage of the coupled oxidation is another multistep process that involves C−C bond breaking and the conversion of the meso-oxygenated heme, $(OEPO)Fe(py)_2$, into the final products, $[(OEOP)Fe^{II}(py)_2]Cl$ and $(OEB)Fe^{III}(py)_2$. In this stage dioxygen, rather than hydrogen peroxide, is the oxidant. $(OEPO)Fe(py)_2$ is very sensitive to dioxygen but less reactive toward hydrogen peroxide. It is likely that this second stage proceeds only after the reductant, hydrazine, is consumed by air oxidation. Any hydrogen peroxide that is formed during the second stage of coupled oxidation may be responsible for the conversion of $[(OEOP)Fe^{II}(py)_2]Cl$ into $(OEB)Fe^{III}(py)_2$. In an independent experiment it has been shown that verdoheme is cleanly converted into $(OEB)Fe^{III}(py)_2$ by treatment with hydrogen peroxide.[6] Unfortunately, no intermediates were observed here during the second stage of coupled oxidation when $(OEPO)Fe^{III}(py)_2$ is converted into the final isolated products. Further work is necessary to understand the mechanism of dioxygen activation in this carbon−carbon bond cleaving process.

It is also important to note that several potential intermediates and products do not appear during the coupled oxidation process. Thus, there is no evidence for the formation of the ferryl ion, in the form of $(OEP)Fe^{IV}O(py)$, in the experiments reported here. Earlier, during work on the spectroscopic characterization of ferryl complexes, this laboratory reported that ferryl porphyrins underwent decomposition to form the ubiquitous μ-oxo iron

(31) Heaton, B. T.; Jacob, C.; Page, C. *Coord. Chem. Rev.* **1996**, *154*, 193.
(32) Audrieth, L. F.; Ogg, B. A. *The Chemistry of Hydrazine*; Wiley: New York, 1951; p 139.
(33) Schmidt, E. W. *Hyrdrazine and Its Derivatives*; Wiley: New York, 1984; p 343.

Scheme 4

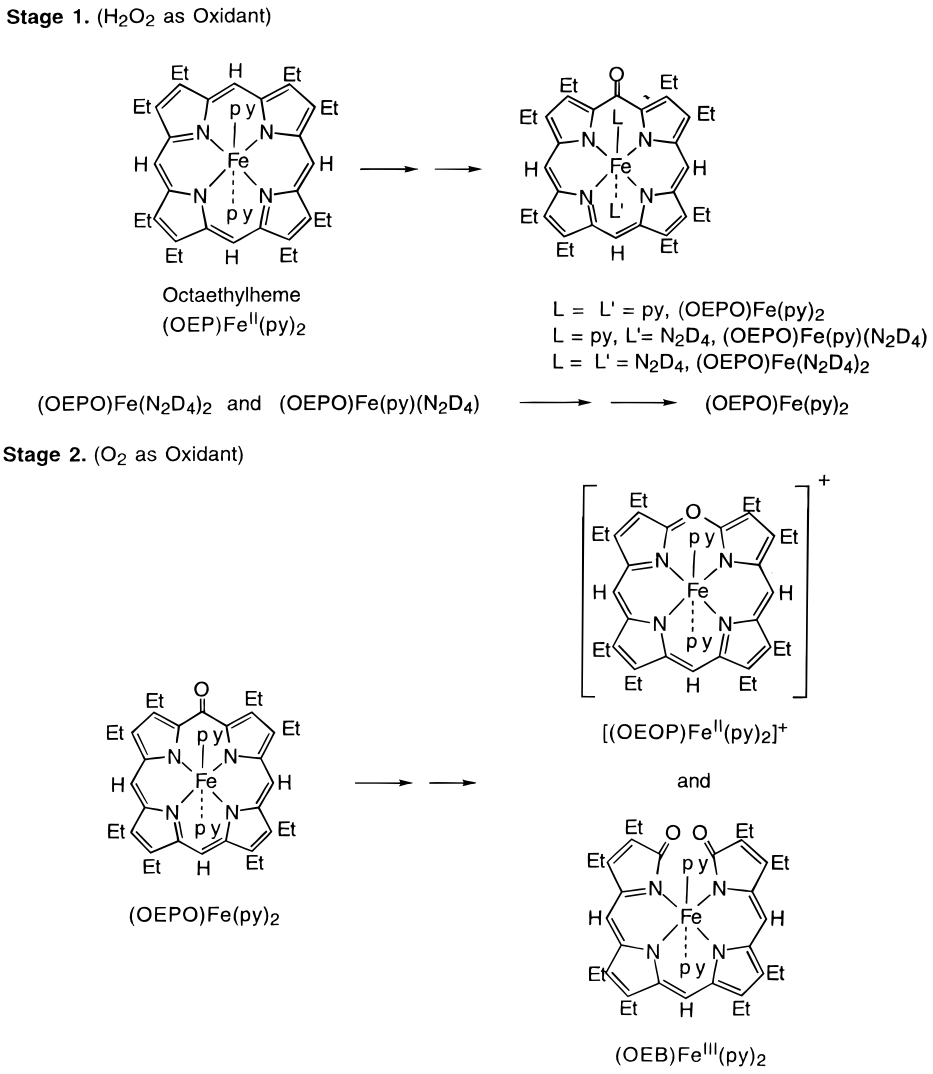

porphyrin dimer, $PFe^{III}OFe^{III}P$.[34,35] After the characterization of verdohemes in this laboratory,[5−7] the decomposition of preformed ferryl complexes was reexamined, and again the μ-oxo iron porphyrin dimer was formed with no evidence for the formation of verdohemes from the ferryl complexes. Complementary experiments also indicated that ferryl ions are not involved in heme catabolism via heme oxygenase.[17] Although $(OEPO)Fe(py)_2$ is capable of undergoing one-electron oxidation to form paramagnetic $[(OEPO)Fe(py)_2]^+$;[25] we cannot say whether this species is present during coupled oxidation. The ^1H NMR spectrum of $[(OEPO)Fe(py)_2]^+$ occurs in the crowded 0−10 ppm region which is obscured by resonances from residual protons in diamagnetic compounds that are involved in this system.[25]

There is also no evidence for attack at more than one meso position of the heme during coupled oxidation. Although iron[36] (and nickel)[37] complexes of *cis*-H_2OEPO_2 and *trans*-H_2OEPO_2 have been characterized so that they could be identified during heme degradation, no evidence for the formation of iron complexes of these ligands has been found in the present set of experiments.

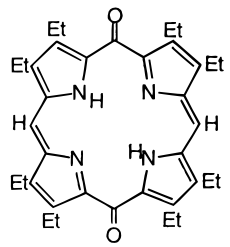

trans-H_2OEPO_2

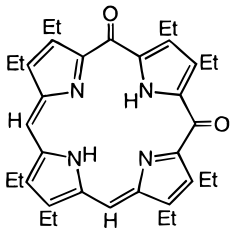

cis-H_2OEPO_2

Experimental Section

Isolation of the Products from the Coupled Oxidation of {(OEP)Fe(py)$_2$}. A 6 μL (0.11 mmol) amount of hydrazine was added to a dioxygen-free sample of 50 mg (0.06 mmol) $\{(OEP)Fe^{II}(py)_2\}$ in a mixture of 50 mL of dichloromethane and 3 mL of pyridine. The sample was cooled in a liquid nitrogen bath until it partly froze. Dioxygen was vigorously bubbled through the slurry. The mixture was stirred and allowed to warm to room temperature under an atmosphere of dioxygen. The mixture, which was initially was red, became green after 20 min of stirring under a dioxygen atmosphere. The green solution was washed with two 100 mL portions of 0.1 N aqueous hydrochloric

(34) Balch, A. L.; La Mar, G. N.; Latos-Grażyński, L.; Renner, M. W.; Thanabal, T. *J. Am. Chem. Soc.* **1985**, *107*, 3003.
(35) Chin, D. H.; Balch, A. L.; La Mar, G. N. *J. Am. Chem. Soc.* **1980**, *102*, 1446.
(36) Balch, A. L.; Noll, B. C.; Olmstead, M. M.; Phillips, S. L. *Inorg. Chem.* **1996**, *35*, 6495.
(37) Balch, A. L.; Noll, B. C.; Phillips, S. L.; Reid, S. L.; Zovinka, E. P. *Inorg. Chem.* **1993**, *32*, 4730.

acid and dried by passage through a 5 cm thick layer of anhydrous sodium sulfate. The volume of the sample was reduced under vacuum until a green precipitate formed. At this stage an additional 20 mL portion of *n*-hexane was added. The green precipitate was collected by filtration and washed with *n*-hexane (yield 26.5 mg, 42%). This solid is the verdoheme analogue, $[(OEOP)Fe^{II}(py)_2]Cl$, which has been characterized previously.[10,26]

The *n*-hexane washings from the procedure described above were combined and evaporated to dryness at room temperature. The dark solid that remained was dissolved in dichloromethane and subjected to chromatography on a 4 × 2 cm silica gel column under dioxygen-free conditions. Elution of the column with dichloromethane produced a reddish band (OEP)FeCl, (yield: 1.7 mg, 4%), which is also observed in the standard coupled oxidation process. Further elution with a dichloromethane/methanol (100:3) mixture produced a green band which was collected and evaporated to dryness to give $\{(OEB)Fe\}_2$ (yield 10.2 mg, 22%).

***In Situ* Monitoring of the Coupled Oxidation Reaction by ^{1}H NMR Spectroscopy.** Coupled oxidation was performed in an NMR tube by a variation on standard routes of verdohemochrome formation.[10,26] A 2.0 μL (0.036 mmol) portion of hydrazine-d_4 (95% in D_2O) was added at −30 °C to a solution of 2 mg (0.003 mmol) of $(OEP)Fe^{II}(py)_2$ in 30 μL of pyridine-d_5 and 200 μL of dichloromethane-d_2. To initiate the reaction, a stream of dioxygen was bubbled through the solution for 45 s at −70 °C.

^{1}H NMR Spectroscopic Monitoring of the Titration of $(OEPO)Fe(py)_2$ with Hydrazine. Titrations were performed through the addition of aliquots of hydrazine-d_4 (95% in D_2O) by means of a microliter syringe to 0.002 mmol of $\{(OEPO)Fe\}_2$ in 300 μL of pyridine-d_5.

Instrumentation. ^{1}H NMR spectra were recorded on a General Electric QE−300 FT spectrometer operating in the quadrature mode (^{1}H frequency is 300 MHz). The spectra were recorded over a 50-kHz bandwidth with 16 k data points and a 10-μs 90° pulse. For a typical spectrum, between 1000 and 5000 transients were accumulated with a 50-ms delay time. The signal-to-noise ratio was improved by the apodization of the free induction decay. The residual ^{1}H resonances of the solvents, chloroform or dichloromethane, were used as a secondary reference.

Electronic spectra were obtained using a Hewlett-Packard diode array spectrometer.

Acknowledgment. We thank the NIH (GM-26226) for financial support.

Supporting Information Available: The UV/vis spectrum of verdoheme (Figure S1), and Curie plots for $(OEPO)Fe(py)(N_2D_4)$ and $(OEPO)Fe(N_2D_4)_2$ (Figures S2 and S3). This material is available free of charge via the Internet at http://pubs.acs.org.

IC981178D